Experimental study on creep and shrinkage of high-performance ultra lightweight cement composite of 60MPa

Kok-Seng Chia[1a], Xuemei Liu[2b], Jat-Yuen Richard Liew[3c] and Min-Hong Zhang[*3]

[1]*Nautic Group Pte Ltd, 300 Beach Road #20-06, The Concourse, 199555, Singapore*
[2]*School of Civil Engineering and Built Environment, Queensland University of Technology, 2 George St, Brisbane, QLD, Australia*
[3]*Department of Civil and Environmental Engineering, National University of Singapore, 1 Engineering Drive 2, Singapore*

Abstract.   Creep and shrinkage behaviour of an ultra lightweight cement composite (ULCC) up to 450 days was evaluated in comparison with those of a normal weight aggregate concrete (NWAC) and a lightweight aggregate concrete (LWAC) with similar 28-day compressive strength. The ULCC is characterized by low density < 1500 kg/m^3 and high compressive strength about 60 MPa. Autogenous shrinkage increased rapidly in the ULCC at early-age and almost 95% occurred prior to the start of creep test at 28 days. Hence, majority of shrinkage of the ULCC during creep test was drying shrinkage. Total shrinkage of the ULCC during the 450-day creep test was the lowest compared to the NWAC and LWAC. However, corresponding total creep in the ULCC was the highest with high proportion attributed to basic creep ($\geq$ ~90%) and limited drying creep. The high creep of the ULCC is likely due to its low elastic modulus. Specific creep of the ULCC was similar to that of the NWAC, but more than 80% higher than the LWAC. Creep coefficient of the ULCC was about 47% lower than that of the NWAC but about 18% higher than that of the LWAC. Among five creep models evaluated which tend to over-estimate the creep coefficient of the ULCC, EC2 model gives acceptable prediction within +25% deviations. The EC2 model may be used as a first approximate for the creep of ULCC in the designs of steel-concrete composites or sandwich structures in the absence of other relevant creep data.

Keywords: cement composite; concrete; creep coefficient; model; shrinkage; ultra lightweight

1. Introduction

Ultra lightweight cement composites (ULCC) (Chia 2011) are characterized by combinations of low densities less than 1500 kg/m^3, and high compressive strengths of about 60 MPa with specific strength up to 47 kPa/kg.m^{-3}. The low density of the ULCC is achieved by using cenospheres obtained from coal-fired thermal power plants as micro-lightweight aggregates. The cenospheres

---

*Corresponding author, Professor, E-mail: mhzhang@nus.edu.sg
[a]Chief Scientist, E-mail: ks.chia@nautic-group.com
[b]Lecturer, E-mail: x51.liu@qut.edu.au
[c]Professor, E-mail: ceeljy@nus.edu.sg

consist of hollow interior covered by thin shell. Their typical particle sizes are between 10 to 300 μm. The ULCC was originally designed for potential structural applications in steel-concrete composites and sandwich structures (Sohel 2012). Due to their low density and low permeability, the ULCC may be used potentially in floating structures where weight of the material is critical.

In structural design for applications in steel-concrete composites or sandwich composites, it is essential to consider the effect of long-term structural response under sustained loading, as the concrete will gradually transfer some of the initial load to the steel due to creep and shrinkage. Depending on exposure environment and type of structure, the concrete in steel-concrete composites may or may not be allowed to dry. For example, when the concrete is used as an in-fill core material such as in composite columns and sandwich slabs, there is limited drying effect. In other configurations, exposure to drying is imminent.

The shrinkage and creep of concrete may lead to cracking caused by stresses developed in concrete due to the restraint of volume change or to loads applied to the structure. According to Kwak *et al*. (2006a, 2006b), such non-structural cracks are related to the material properties of concrete and construction practices, and a number of factors can concurrently contribute to the occurrence of such cracks.

In this study, shrinkage and creep behaviour of a ULCC are evaluated and compared with those of a normal weight aggregate concrete (NWAC) and a lightweight aggregate concrete (LWAC) with similar 28-day compressive strength. Terms relating to creep and shrinkage are shown in Fig. 1 (ACI 209 2005). Concrete undergoes autogenous shrinkage (before drying) and drying shrinkage. Upon loading, drying creep and basic creep (creep without drying effect) occur.
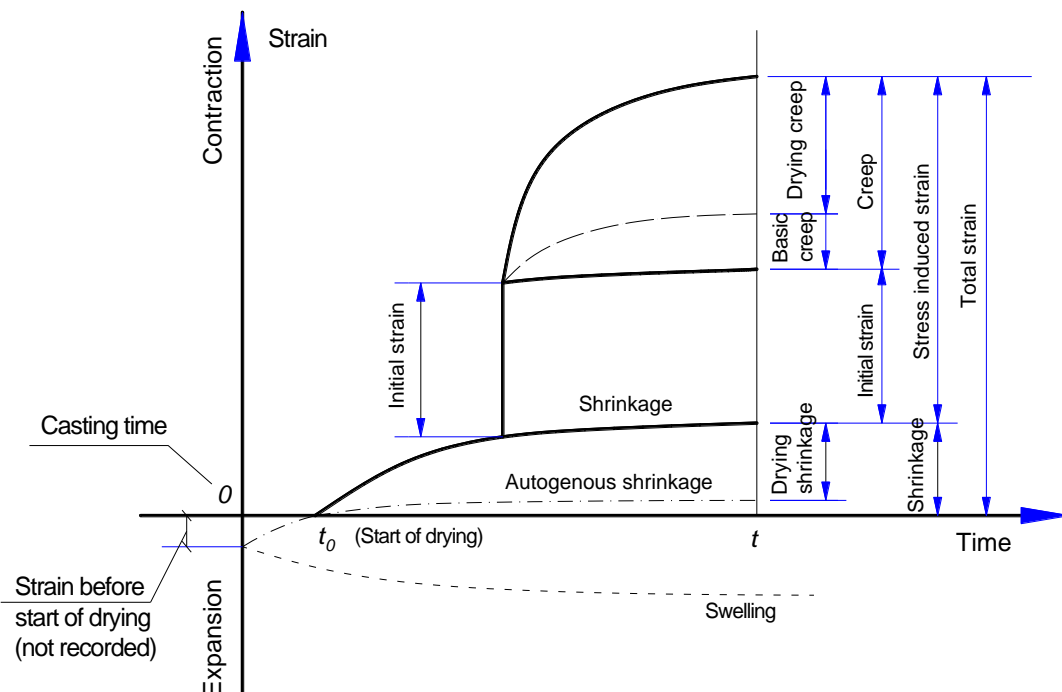

Fig. 1 Relationship between various measured and derived strains in concrete under sustained loading (ACI 209 2005)

Table 1 Mixture proportions

Type	w/cm	Mixture proportion (by mass)* $W : (C+S) : FA : CA$	Fiber (vol. %)	Cementitious paste content (vol. %)	Flow (mm)	Slump (mm)
ULCC	0.35	0.35 : (0.92 + 0.08) : 0.42 : 0	0.9	52	200	--
LWAC	0.35	0.35 : (0.92 + 0.08) : 1.59 : 0.82	0	35	--	90
NWAC	0.45	0.45 : 1.00 : 1.57 : 2.57	0	32	--	100

* W – water, $C+S$ – cement and silica fume, FA – fine aggregate (quartz sand for LWAC & NWAC, lightweight filler for ULCC), CA – coarse aggregate (granite for NWAC, expanded clay lightweight aggregate for LWAC).

The shrinkage and creep of the concretes were determined at an environment of $28\pm1^{\circ}$C and $66\pm4\%$ relative humidity (RH). For creep test, sustained loads at 40% of compressive strengths of the ULCC, LWAC, and NWAC determined at the age of creep test were applied on concrete specimens. Results are analyzed and discussed. Creep coefficient predicted by five models based on equations from ACI, CEB-FIP, Eurocode 2 and literature are compared with experimental values and discussed.

2. Experimental details

Mixture proportions of the ULCC and two other control concrete mixtures – LWAC and NWAC - are shown in Table 1 by mass. The water to cementitious material ratio (*w/cm*) was 0.35, 0.35, and 0.45 for ULCC, LWAC, and NWAC, respectively. The ULCC was fibre-reinforced to reduce brittleness, using polyvinyl alcohol (PVA) fibres with a length of 6 mm, a diameter of 27 μm, and a specific gravity of 1.30. The fibres had a tensile strength of 1600 MPa, an elastic modulus of 39 GPa, and an elongation of 7 %. The NWAC and LWAC with similar 28-day compressive strengths were prepared for comparison. The NWAC contained crushed granite with a max size of 20 mm. The LWAC contained expanded clay lightweight aggregate (LWA) with sizes of 4-8 mm (Fig. 2). Cenospheres are used as micro-lightweight aggregates for the ULCC, as shown in Fig. 2. Silica fume of 8% by mass of total cementitious material was used in the ULCC and LWAC for strength enhancement. Since the ULCC has no coarse aggregate, a flow test generally used for mortar was adopted to evaluate its workability. The ULCC had good flowability with a flow value of 200 mm (Table 1). The LWAC and NWAC had slumps of 90 and 100 mm, respectively.

Specimens ($\varnothing$ 150 by 300 mm cylinders) were prepared for various tests as shown in Table 2. The autogenous shrinkage was measured by a modified ASTM C426 (2010) method. Instead of using gauge plugs together with a comparator to measure the shrinkage as specified in the standard, an alternative method was adopted in this study for shrinkage measurement by using mechanical (demec) gauges. After de-moulding, specimens for autogenous shrinkage test were fixed with demountable mechanical (demec) gauges for strain measurement, and then coated and sealed with epoxy and allowed to dry overnight, before being further sealed with adhesive aluminium tape. Measurement for the autogenous shrinkage started as soon as the specimens were sealed with aluminium tape, typically 2-3 days after casting.

The rest of specimens were moist-cured for 7 days (NWAC and LWAC) or 14 days (ULCC) before being exposed to laboratory air at 28 $^{\circ}$C and about 66% RH. The length of moist-curing for

each mixture type was selected to simulate typical applications in practice. The NWAC and LWAC are typically used in exposed structures while the ULCC is intended for use in enclosed sandwich composite structures which limit the external exposure to environment.

Total shrinkage was determined by a modified ASTM C 426 (2010) method and the modification is the same as for the autogenous shrinkage measurement, while creep was determined with reference to ASTM C512/512M (2010). At the start of air drying, the specimens for creep and total shrinkage tests were fixed with demec gauges using fast-setting epoxy. Measurement for the total shrinkage started as soon as the specimens were fixed with demac gauges, typically on the same day after removal from the moist-curing room. Specimens for basic creep test were coated with epoxy and sealed with aluminium tape.

At the age of 28 days, compressive strength and elastic modulus were determined. The creep specimens were loaded to 40% of the compressive strength using hydraulically controlled creep frame of 800 kN capacity (Fig. 3). Due to stress reduction caused by drying shrinkage and stress relaxation of the specimens under sustained load, the initial applied load would decrease over time. However, each of the creep frames is controlled individually with pressure sensor to maintain the applied load to within 2% of present level with automatic adjustments using hydraulic pump.

Table 2 Details of test specimens

Test	No. of specimens	Specimen size, mm	Specimen details
Basic creep	3		Fixed with demec gauges and sealed using epoxy and aluminium tape
Total creep	3	150×300 cylinders	Fixed with demec gauges
Autogenous shrinkage	3		Fixed with demec gauges and sealed using epoxy and aluminium tape
Total shrinkage	3		Fixed with demec gauges
Compressive strength	3	150×300 cylinders	--
Elastic modulus	3*	150×300 cylinders	--

*Total creep specimens were used for determining elastic modulus.

Expanded clay LWA   Cenosphere

Fig. 2 Lightweight aggregates used for LWAC and ULCC
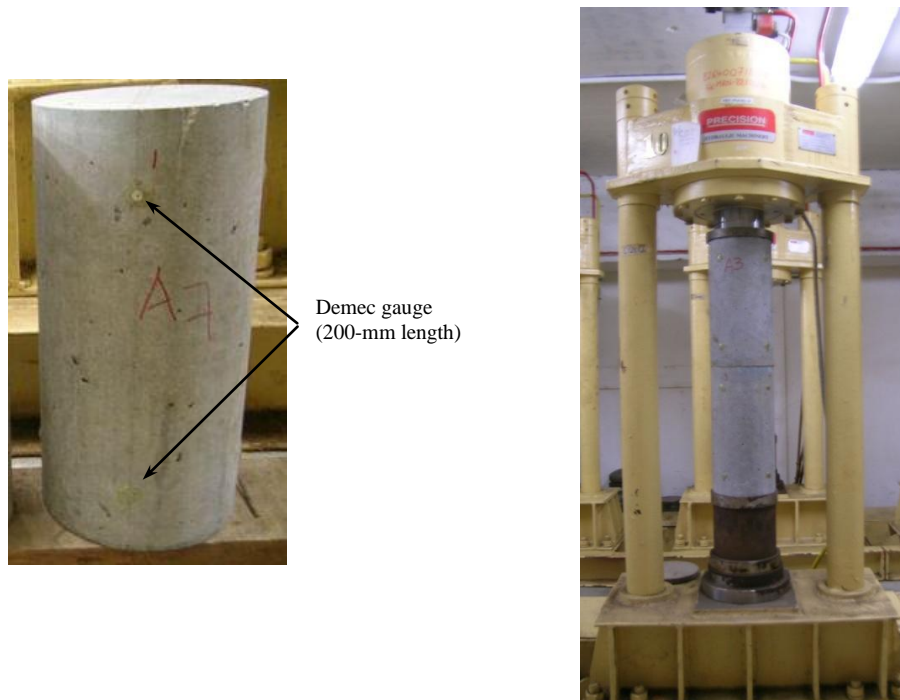
Fig. 3 Test specimen (Ø 150 by 300 mm cylinder) showing a set of demec gauge (left) and hydraulically controlled creep frame with 2 test specimens (right)

3. Results and discussion

3.1 Basic material properties

Table 3 shows basic material properties and experimental results on shrinkage and creep. Densities of the fresh ULCC, LWAC, and NWAC were about 1450, 1850, and 2350 kg/m^3, respectively. The 28-day compressive strength (f_c') of both ULCC and LWAC were about 60 MPa while NWAC was 50 MPa. Elastic modulus (E_c) of the ULCC, LWAC, and NWAC were 15, 23, and 26 GPa, respectively. The elastic modulus of the NWAC was lower than expected for a concrete with *w/cm* of 0.45, which indicated that the granite aggregate used in the NWAC probably had low elastic modulus.

3.2 Elastic and time-dependent deformations

3.2.1 Elastic strain

The short-term strain at the moment of loading is termed initial strain and is frequently considered as a nominal elastic strain. For sustained loading at 40% of compressive strength, the ULCC had the highest initial elastic strain, followed by the LWAC and NWAC, respectively (Table 3). The elastic strain is inversely proportional to the elastic modulus, and was determined within 15 minutes after loading the creep specimens. Results are expected based on the elastic modulus of the respective mixture types.

Table 3 Material properties and summary of creep and shrinkage results

| Type	Unit weight, kg/m^3	f_c', MPa	E_c, GPa	Moist-curing, days	Total shrinkage* $\mu\varepsilon$	Total shrinkage**, $\mu\varepsilon$	Load age, days	Load level, % f_c'	Load level, MPa	Elastic strain, $\mu\varepsilon$	Creep duration, days	Specific creep***, $\mu\varepsilon$/MPa	Creep coefficient ***	Total Creep, $\mu\varepsilon$	Basic Creep, $\mu\varepsilon$
ULCC	1,450	61.7	15.2	14	120	25	28	40	24.7	1700	7	20	0.30	500	490
					145	45					28	35	0.50	835	795
					180	90					91	50	0.73	1240	1155
					275	180					364	75	1.10	1870	1685
					310	215					450	77	1.12	1900	1765
LWAC	1,850	63.4	23.4	7	105	<5	28	40	25.4	1100	7	13	0.29	320	280
					125	15					28	18	0.42	460	385
					155	75					91	26	0.60	655	565
					355	235					364	42	0.95	1040	750
					380	270					450	42	0.95	1060	755
NWAC	2,350	50.0	26.2	7	275	40	28	40	20.0	750	7	22	0.60	445	320
					390	125					28	38	1.01	760	525
					535	270					91	57	1.51	1130	725
					645	375					364	78	2.09	1550	1180
					650	380					450	80	2.12	1590	1225

* included strains developed prior to the creep test

** did not include shrinkage strains developed prior to the creep test

*** based on total creep strain
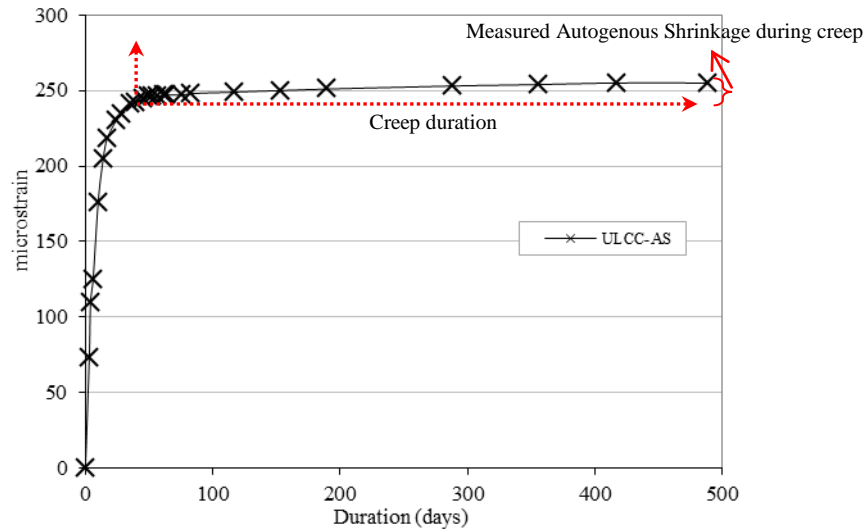
(a) 3 days to the end of creep test
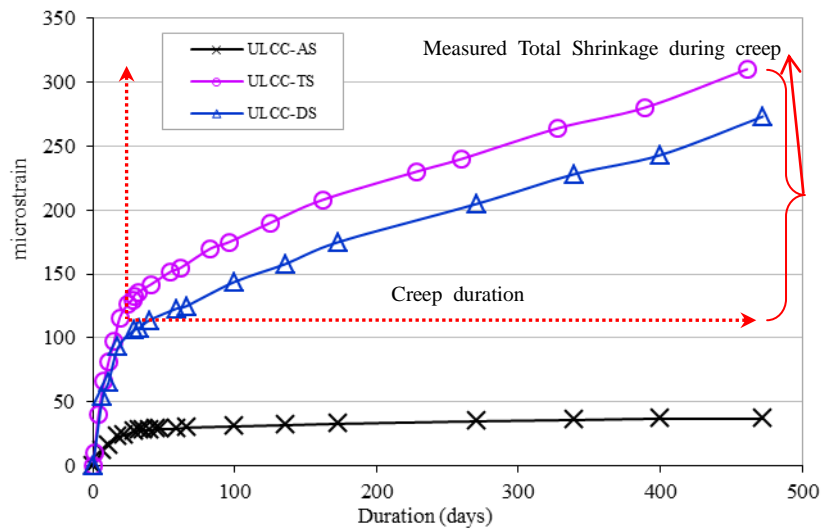
(b) 16 days to the end of creep test

Fig. 4 Autogenous and total shrinkages for ULCC plotted from different starting time

3.2.2 Shrinkage strain

Total shrinkage strain was obtained from the measurement of exposed load-free specimens starting at the age of 16 days for the ULCC and 8 days for the NWAC and LWAC. Autogenous shrinkage strain is obtained from measurement of sealed load-free specimens starting at the age of 3 days for the ULCC and 2 days for both NWAC and LWAC. The difference between the total shrinkage and autogenous shrinkage is assumed to be drying shrinkage.

Fig. 4 shows shrinkage strains of the ULCC plotted from different starting times. Overall autogenous shrinkage of the ULCC from 3 days to the end of the creep test was about 250 $\mu\varepsilon$.
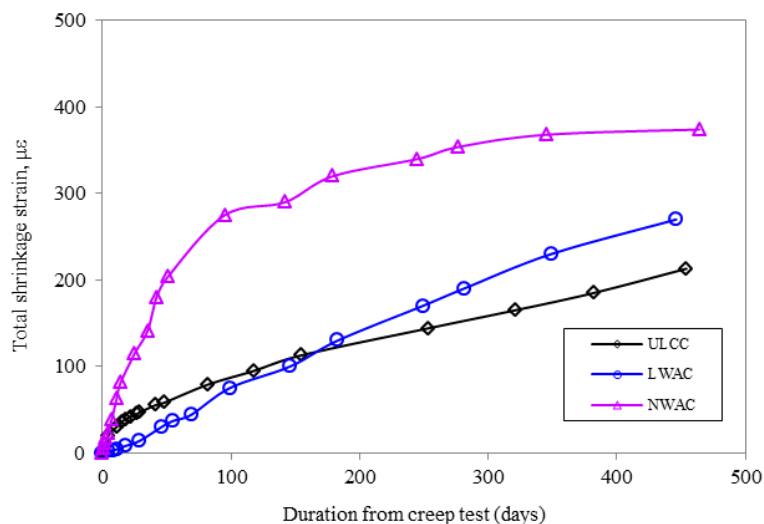
Fig. 5 Total shrinkage strain of the ULCC in comparison to that of the LWAC and NWAC during the creep test

From Fig. 4(a) it is observed that the autogenous shrinkage increased rapidly at early age and almost 95% of the autogenous shrinkage occurred before the start of the creep test at 28 days.

From Fig. 4(b), overall total shrinkage for the ULCC measured from the age of 16 days (after 14 days of moist-curing) to the end of the creep test was about 300 με, from which about 200 $\mu\varepsilon$ occurred during the creep test. From the figure it is clear that majority of the shrinkage occurred during the creep test was drying shrinkage.

The total shrinkage during the creep test was in the ascending order of LWAC, ULCC and NWAC before 180 days (Fig. 5). Beyond 180 days, the total shrinkage was in the ascending order of ULCC, LWAC and NWAC. The lower total shrinkage of the LWAC compared with the ULCC prior to 180 days might be attributed to water absorbed inside the LWA which provided internal curing (Bentz 2011). The higher total shrinkage of the NWAC during the creep test period was probably due to its higher *w/cm* without silica fume compared with the ULCC and LWAC. As shown in Fig. 5, the total shrinkage of NWAC approached asymptotical value of about $370\mu\varepsilon$ at about 240 days of creep test, whereas the total shrinkage of the ULCC and LWAC continued to increase up to 450 days though with lower values.

3.2.3 Creep strain, specific creep, and creep coefficient
Creep strain

Total creep strain is obtained from total strain subtracting initial elastic strain and total shrinkage strain. Developments of total creep and total shrinkage strains from the start of creep loading for the ULCC, LWAC, and NWAC are presented in Fig. 6 (a), (b), and (c). From the figures it is observed that the creep strain is in the ascending order of LWAC, NWAC and ULCC. At 450 days under sustained load, the ULCC had total creep strain about 80% and 20% higher than the LWAC and NWAC, respectively. The shrinkage strain is generally much lower than that of the creep strain. The high creep strain in the ULCC is likely due to its low elastic modulus related to a

porous structure due to the hollow ecospheres.

The total creep consists of basic creep and drying creep. From Fig. 6 (d), (e), and (f), it is observed that the ULCC had high basic creep (≥ ~90%), but low drying creep, relative to total creep. For the LWAC, the proportion of basic to total creep was ~85% up to 91 days of the creep test. After 1 year and beyond, the proportion of the basic creep to total creep decreased to about 70%, whereas the proportion of drying creep to total creep increased correspondingly from ~15% at 91-day to ~30% at 450-day creep test. The initial lower drying creep up to 91 days was likely due to internal curing in the LWAC mentioned earlier, mitigating the effect of drying. The proportion of the basic creep relative to total creep in the NWAC was between 65-75% throughout the creep test period.

Comparison of the creep strains between the 3 types of the mixtures is shown in Fig. 7. The ULCC had the highest total creep and basic creep, followed by the NWAC and then LWAC, at the same age of creep loading (Table 3 and Fig. 7). The NWAC had the highest drying creep.

Specific creep

Research has shown that creep of both lightweight and normal weight concretes is proportional to the applied stress up to approximately 60% of its strength. Superposition therefore applies and calculation can be based on specific creep which relates the creep strain to the unit of applied stress (CEB/FIP 1983). The specific creep (or creep) is dependent on numerous factors including sustained load level, maturity of concrete at the age of loading, environmental condition, specimen size, initial compressive strength and elastic modulus, rate of strength development etc.

Fig. 8 shows that the specific creep of the ULCC is similar to that of the NWAC. However, the specific creep of the LWAC is the lowest (about 50-60% that of the ULCC and NWAC) throughout the test period. At 450 days the specific creeps of the LWAC, ULCC, and NWAC were 42, 77, and 80 με/MPa, respectively (Table 3). The specific creep results of the NWAC and LWAC are consistent with data from CEB/FIP (1983) and a study on LWAC by Lopez (2004). Data from CEB/FIP (1983) shows that final specific creep of LWAC with similar strength as the LWAC in current study at the time of loading ranged between 50 to 60 με/MPa. In general the specific creep reaches the final value after 2-5 years for NWAC and LWAC (CEB/FIP 1983). In the study by Lopez (2004), the LWAC was loaded at 24 hrs to 40% of 24-hr compressive strength (67.3 MPa) which was similar to the 28-day strength of the LWAC in current study. Results from that study were similar to the LWAC in current study as the 450-day specific creep was about 43 με/MPa and creep coefficient was about 1.0. Despite the fact that the loading age was different for the two studies (24 hrs vs. 28 days), the two LWACs had similar strength at loading, and subsequently similar specific creep and creep coefficient.

The cement paste matrix affects the creep of concrete. Higher volume and lower strength of cement paste increases creep. While the quantity of paste content is similar in the LWAC and NWAC (32-35%) in current study (Table 1), their quality differed. The LWAC with silica fume and lower *w/cm* had denser paste with higher strength and lower porosity compared with the NWAC. In spite of the lower elastic modulus of the LWA in comparison to the granite aggregate in the NWAC, the LWAC had lower 450-day specific creep and creep strains compared with the NWAC. This implies that quality of the paste, in terms of the porosity and strength which is influenced by water-to-cementitious material ratio and use of silica fume, is a more dominant factor than the stiffness of the aggregate comparing these two concretes. It is also likely that the paste matrix in the LWAC benefited from the internal curing with further access to additional water released from the pre-soaked LWA after the initial curing period (Bentz 2011).

Creep coefficient

Creep coefficient is a ratio of total creep strain to elastic strain, and is a dimensionless quantity. Data of the creep coefficient are shown in Table 3 and Fig. 9. The creep coefficient of the ULCC at early-age loading within 7 days is similar to that of the LWAC. After that, the creep coefficient of the ULCC is about 18-20% higher than that of the LWAC. The NWAC had the highest creep coefficient, exceeding 2.0 after about 1-year creep test. This is twice as high as the LWAC and about 80% higher than the ULCC. This may be partly attributed to the lower compressive strength of the NWAC compared with the ULCC and LWAC. While it is expected that the creep coefficient increases as compressive strength decreases (Lopez 2004), it is not easy to predict the extent of the change accurately. Typical long-term creep coefficient for NWAC ranges from 1.2 (very low creep) to 6.0 (very high creep) (ACI 209 2005).

3.3 Creep predictions

Due to time-consuming nature of shrinkage and creep tests, creep models have been developed to predict these time-dependent properties. These models include ACI 209R-92 (ACI 209 1992), CEB MC90-99 (CEB 1999), CEB MC90 (CEB 1993), Eurocode 2 – Annex B (EC2) (BSI 2004), and GL2000 (Gardner 2004). In these models, stress-dependent strain is presented in the form of a compliance function

$$J(t, t_0) = 1/E_{cmt0} + \varphi(t, t_0)/E_{cmt} \tag{1}$$

where $J(t, t_o)$ is compliance of concrete loaded at age t_o at time t ($t_o = 28$ days in this study), E_{cmt0} is the elastic modulus at loading age t_o, E_{cmt} is elastic modulus at age t, and $\varphi(t, t_o)$ is the creep coefficient of concrete loaded at the age t_o at time t. The compliance represents the total stress-dependent strain per unit stress applied. The first term in the above equation is instantaneous elastic strain which is obtained in about 10^{-9} second in theory (ACI 209 2008). The second term is the creep strain from the start of loading at the age of t_o. In this study, the measured creep coefficient $\varphi(t, t_o)$ is compared to predicted values from the models which are independent of the elastic modulus.
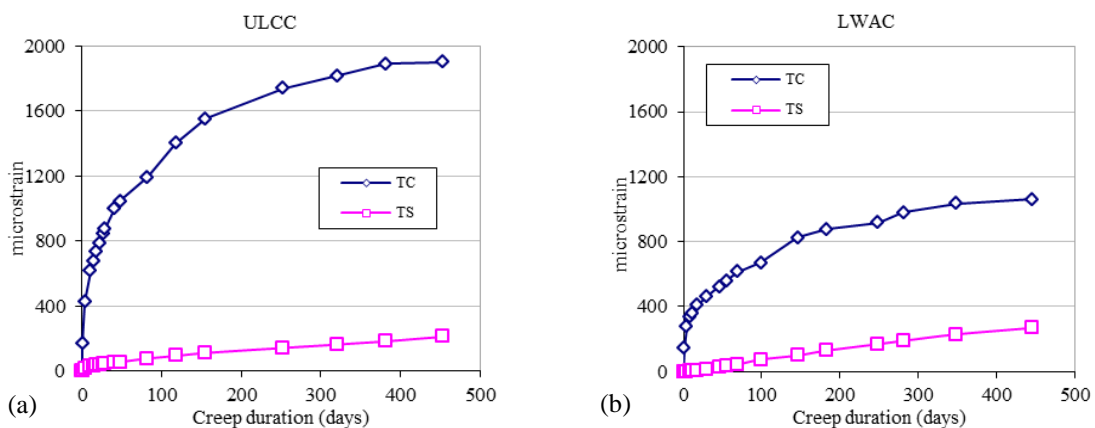

Fig. 6 Total shrinkage strain of the ULCC in comparison to that of the LWAC and NWAC during the creep test (TC – total creep, TS – total shrinkage, BC – basic creep, DC – drying creep)
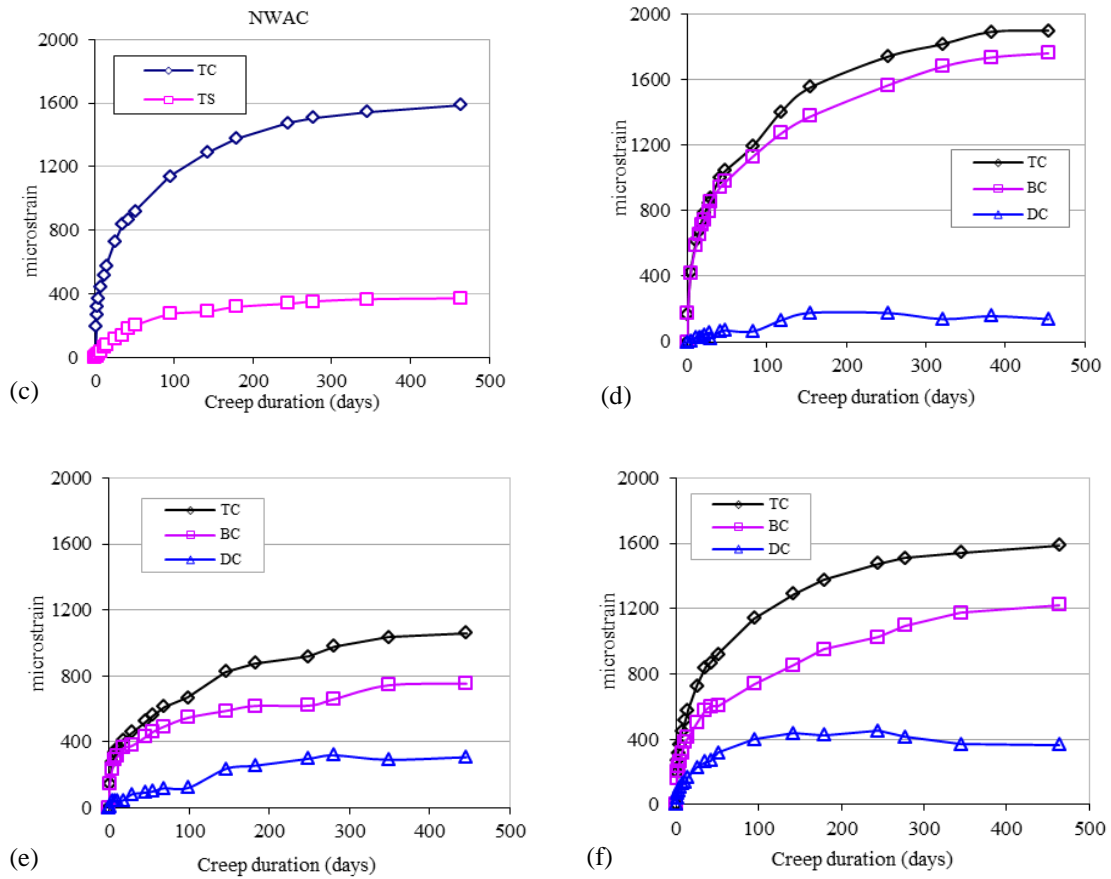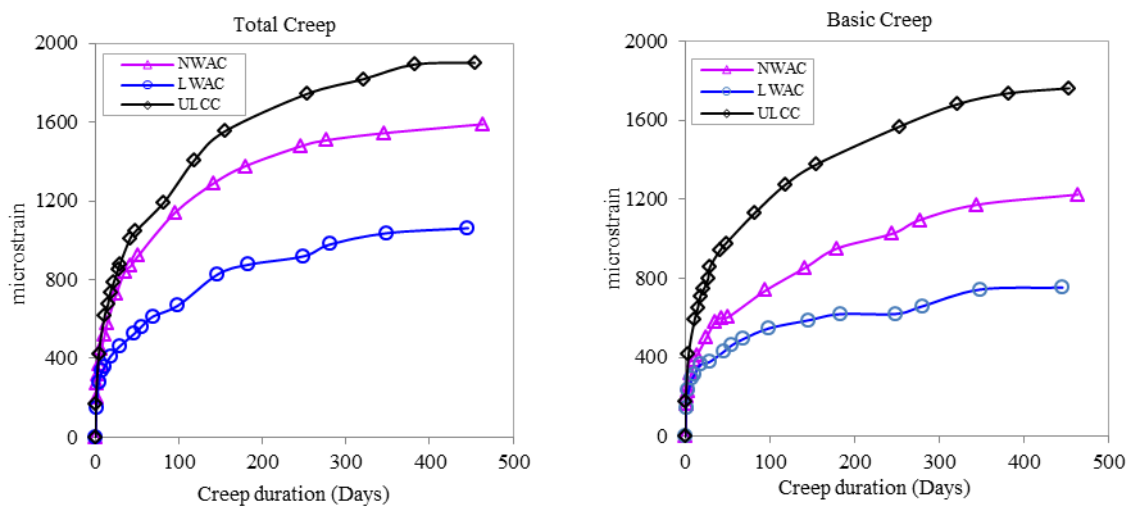
Fig. 6 Continued

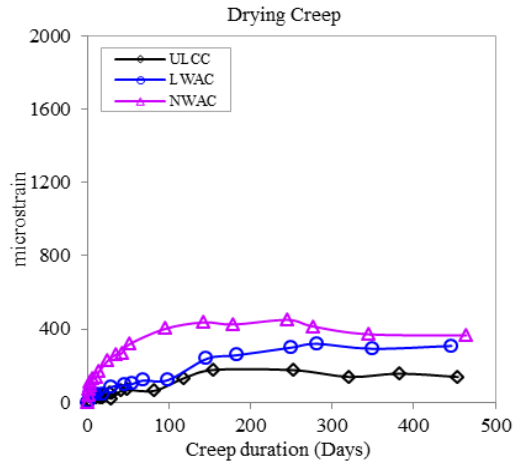Fig. 7 Creep strains (total ,basic and drying) of ULCC, LWAC and NWAC
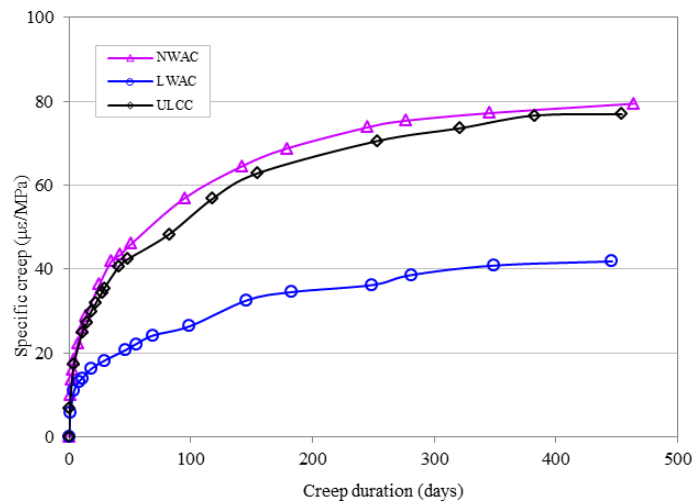
Fig. 7 Continued

Fig. 8 Specific creep of the ULCC, LWAC, and NWAC

The models and main parameters used in the various models for the prediction of the creep coefficients are shown in Table 4. Common assumptions of the above models include the use of ASTM Type I or III cements, relative humidity from 40-100%, at least one day of moist-curing (CEB models have a limit of maximum 14 days), and greater than one day of loading age (ACI model has a limit of minimum 7 days). Maximum applicable stress-strength ratio at age of loading is between 0.4 and 0.5 for the models considered. Also, the models were established with concretes of typical composition without silica fume, fly ash larger than 30% or other natural pozzolans. Typical applicable range of compressive strength is between about 15 and 90 MPa based on 28-day cylinder strength, except for CEB MC90 where an upper limit of 120 MPa is specified.

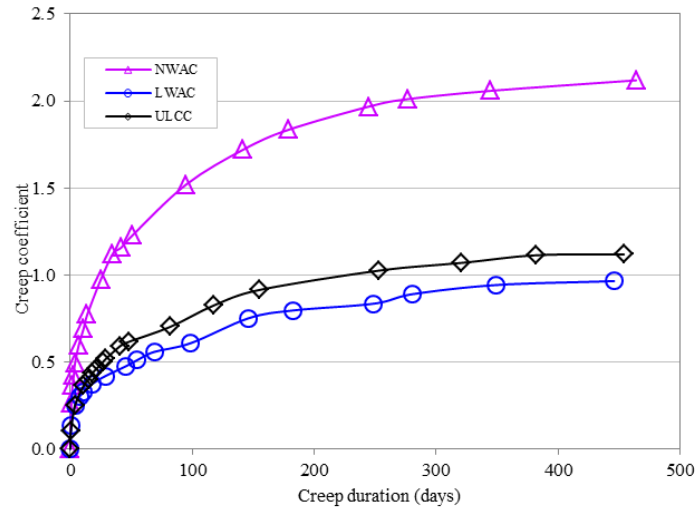The ACI 209R-92 model is an empirical model (Branson 1971) based on the principle of a

Fig. 9 Creep coefficients of the ULCC, LWAC, and NWAC

hyperbolic curve that tends to an asymptotic ultimate creep value (or creep coefficient) in time. The CEB MC90 model has similar concept as the ACI 209R-92 model as it gives a hyperbolic change with time for creep prediction. The CEB MC90-99 model includes the latest improvements to the CEB MC90 model and also takes into account particular characteristics of high-strength concretes and allows for effect of high stresses exceeding 0.4, up to 0.6 of stress-strength ratio. The EC2 model is in general similar to the CEB MC90 and CEB MC90-99 models with some exceptions such as no consideration of temperatures beyond the standard 20°C and limit of stress-strength ratio to 0.4. The GL2000 model included minor modifications to some coefficients and strength development equation of their original model which was influenced by the CEB MC90 model.

Experimental data of creep coefficient are compared with predicted values from each of the five creep models mentioned earlier and results are shown in Fig. 10. The measured creep coefficients are based on total creep results, except for comparison with GL2000 whereby the measured creep coefficients based on basic and drying creep are also compared. These are being referred to as 'basic creep coefficient' and 'drying creep coefficient' in the discussion.

In Fig. 10, other than the unity line, there are two pairs of lines representing deviation from unity by ±25% for the nearest pair to ±50% for the furthest pair. For design purposes, ACI 209.2R-08 states that an accuracy of ±30% for compliance prediction would be adequate, although improvement by up to 5% would be excellent. This implies that prediction of creep coefficient within ±25% would be acceptable for design purpose.

The five creep models in this study tend to over-estimate the creep coefficient of the ULCC and LWAC. Among the 5 models, the EC2 model gives acceptable prediction within +25% deviations for the entire range of creep coefficients of the ULCC. This model also gives reasonably good prediction within +25% deviations for the LWAC with creep coefficients greater than 0.6, and between +25 to +50% deviations for coefficient less than 0.6. On the other hand, most of the models tend to under-estimate creep coefficient of the NWAC. This may be related to the low elastic modulus as mentioned earlier. The best models which provide prediction within ±25%

deviations for the NWAC are the CEB MC90 and CEB MC-90-99 models.

Prediction of basic creep coefficient for the three mixtures by GL2000 model is similar to the total creep coefficient. The GL2000 model tends to over-estimate for the ULCC and LWAC, but under-estimates for the NWAC. For both basic and total creep coefficients of the ULCC, the

Table 4 Main parameters used in the various models for prediction of the creep coefficients

ACI 209R-92 model $\quad \emptyset(t,t_0) = \dfrac{(t-t_0)}{f+(t-t_0)} \emptyset_u \gamma_{RH} \gamma_{vs} \gamma_{t0}$	$f = 26e^{\{1.42 \times 10^{-2}(\frac{V}{S})\}}$

Correction Factors

γ_{RH}=1.27−0.67h for h≥0.40	$\gamma_{vs} = \dfrac{2}{3}(1+1.13e^{\left\{-0.0213(\frac{V}{S})\right\}})$	γ_{t0}=1.25$t_o^{-0.118}$

$\emptyset(t, t_o)$ is creep coefficient at concrete age t due to a load applied at age t_o (28 days in this study); t_o is age at start of creep test; $(t - t_o)$ is duration of creep load test; f is related to a given member shape and size that define the time-ratio part; (V/S) = 37.5 for a specimen cylinder size of 150 by 300 mm; $\emptyset_u$ is ultimate creep coefficient (equals to 2.35); γ $(_{RH / vs / t_o})$ are correction factors for relative humidity, member geometry and curing condition respectively; h is relative humidity in decimals (0.65 in this study).

CEB MC90-99 model

$\emptyset(t,t_o)=\emptyset_o\beta_c(t-t_o)$; $\emptyset_o=\emptyset_{RH,T}\beta(f_{cm28})\beta(t_o)$; $\beta_c(t-t_o)=[\dfrac{(t-t_o)}{\beta_{H,T}+(t-t_o)}]^{0.3}$

$\emptyset_{RH,T}=\emptyset_T+[\emptyset_{RH}-1]\emptyset_T^{1.2}$; $\emptyset_T=e^{[0.015(T-20)]}$; $\beta_{H,T}=\beta_H\beta_T$

$\emptyset_{RH} = [1 + \dfrac{1-h}{\sqrt[3]{0.1\left[\frac{(\frac{V}{S})}{50}\right]}}\alpha_1]\alpha_2$ $\qquad$ $\beta(f_{cm28}) = \dfrac{5.3}{\sqrt{f_{cm28}/10}}$ $\qquad$; $\qquad$ $\beta(t_o) = \dfrac{1}{0.1+t_o^{0.2}}$

$\beta_H = 150[1 + (1.2h)^{18}](\dfrac{V}{S}) + 250\alpha_3 \le 1500\alpha_3$ $\qquad\qquad$;

$\beta_T = e^{[\frac{1500}{273+T}-5.12]}$

$\alpha_1 = [\dfrac{35}{f_{cm28}}]^{0.7}$; $\alpha_2 = [\dfrac{35}{f_{cm28}}]^{0.2}$; $\alpha_3 = [\dfrac{35}{f_{cm28}}]^{0.5}$

$\emptyset_o$ is notional creep coefficient; f_{cm28} is mean compressive strength at age 28 days; T is creep test temperature (28 °C in this study).

For **CEB MC-90 model**, the equations are similar to CEB MC90-99, except the values of α_1, α_2, and α_3 are taken as 1.0.

For **EC2 model**, the equations are similar to CEB MC90-99, except there is no adjustment for effect of temperatures beyond 20 °C. Hence, $\emptyset_{RH}$ is used in place of $\emptyset_{RH,T}$ to calculate notional creep coefficient, and β_H is used in place of $\beta_{H,T}$ to calculate $\beta_c(t - t_o)$.

GL2000 model

$\emptyset(t, t_o) = \emptyset(t_c)[2\dfrac{(t-t_o)^{0.3}}{(t-t_o)^{0.3}+14} + (\dfrac{7}{t_o})^{0.5}(\dfrac{(t-t_o)}{(t-t_o)+7})^{0.5} + 2.5(1 - 1.086h^2)(\dfrac{(t-t_o)}{(t-t_o)+77(V/S)^2})^{0.5}]$

First two terms calculates the basic creep and the third term is for drying creep.

$\emptyset(t_c) = [1 - (\dfrac{(t_o - t_c)}{(t_o - t_c) + 0.12(\frac{V}{S})^2})^{0.5}]^{0.5}$

$\emptyset(t_c)$ is correction term for effect of drying before loading; t_c is age of concrete where moist-curing ends in days (equals 14 days for ULCC and 7 days for NWAC and LWAC).
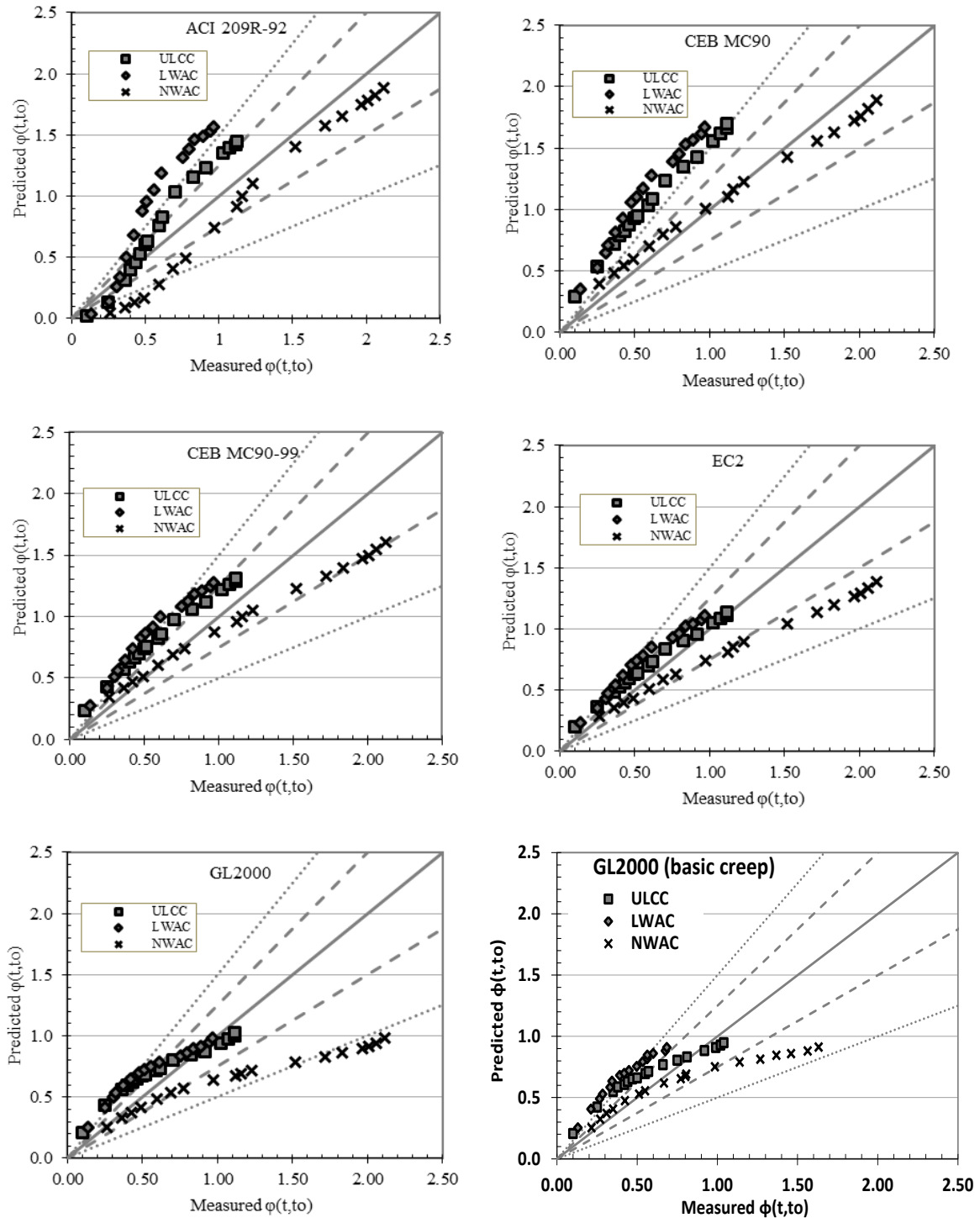
Fig. 10 Comparison of predicted creep coefficients from models with experimental data (Dashed lines is ±25% and dotted lines are ±50% deviation from unity)
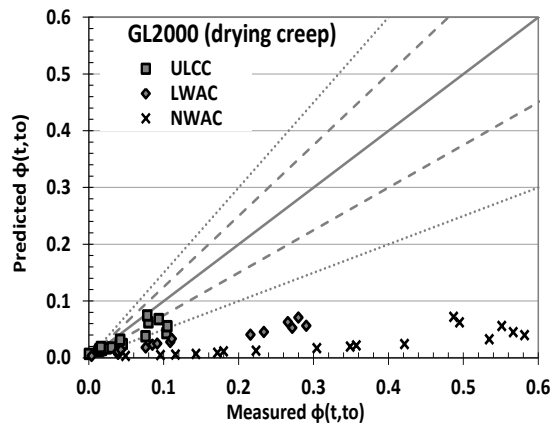
Fig. 10 Continued

prediction is within +25% deviations relative to the measured creep coefficients greater than 0.5 to the upper limit obtained in this study (about 1.0). This is likely due to the fact that drying creep constituted only a small proportion (less than 8%) of the measured total creep for the ULCC, and the prediction of the drying creep coefficient for the ULCC by the GL2000 model is largely within ±50% deviations. However, drying creep coefficients of the LWAC and NWAC are greatly under-estimated by the GL2000 model.

4. Conclusions

Creep and shrinkage of ultra lightweight cement composite (ULCC) up to 450 days are evaluated in this study compared with a lightweight aggregate concrete (LWAC) and a normal weight concrete (NWAC) of comparable 28-day compressive strength. Based on the results, the following conclusions can be drawn:

• Autogenous shrinkage increased rapidly in the ULCC at early-age and almost 95% occurred prior to the start of creep test at 28 days. Majority of the shrinkage occurred during the creep test of the ULCC was drying shrinkage. The total shrinkage during the creep test was in the ascending order of LWAC, ULCC and NWAC before 180 days. Beyond 180 days, the total shrinkage was in the ascending order of ULCC, LWAC and NWAC. The lower total shrinkage of the LWAC compared with the ULCC prior to 180 days might be attributed to water absorbed inside the LWA which provided internal curing.

• Creep strain is in the ascending order of LWAC, NWAC and ULCC. At 450 days the ULCC had total creep strain about 80% and 20% higher than the LWAC and NWAC, respectively. The ULCC had high basic creep (more than 90%) relative to total creep. For the LWAC, the proportion of basic creep to total creep was about 70% at 450 days. The proportion of basic creep to total creep for the NWAC was between 65-75% throughout the creep test.

• The shrinkage strain is generally much lower than that of the creep strain for the 3 types of the concretes subjected to sustained loading in about 66% RH environment.

• The specific creep of the ULCC at 450 days was similar to that of the NWAC, but more than 80% higher than the LWAC. The 450-day creep coefficient of the ULCC was about 47% lower

than that of the NWAC and about 18% higher than that of the LWAC.

 • Five creep models evaluated in this study tend to over-estimate the creep coefficient of the ULCC. The EC2 model provides acceptable prediction within +25% deviations for the entire range of creep coefficients of the ULCC. Hence, based on the limited results from this study, the EC2 model may be used as a first approximate for the creep of ULCC in the designs of steel-concrete composites or sandwich structures in the absence of other relevant creep data.

Acknowledgments

References

ACI 209 (1992), *Prediction of creep, shrinkage, and temperature effects in concrete structures*, ACI 209R-92, American Concrete Institute, Farmington Hills.

ACI 209 (2005), *Report on Factors Affecting Shrinkage and Creep of Hardened Concrete*, American Concrete Institute ACI 209.1R-05.

ACI 209 (2008), *Guide for Modeling and Calculating Shrinkage and Creep in Hardened Concrete*, ACI 209.2R-08, American Concrete Institute, Farmington Hills.

ASTM C426-10 (2010), *Standard test method for linear drying shrinkage of concrete masonry units*, ASTM international, West Conshohocken (PA).

ASTM C512/C512M-10 (2010), *Standard test method for creep of concrete in compression,* ASTM international, West Conshohocken (PA).

Bentz, D.P. and Weiss, W.J. (2011), "Internal Curing: A 2010 State-of-the-Art Review," *National Institute of Standards and Technology*, NISTIR 7765.

Branson, D.E. and Christiason, M.L. (1971), "Time Dependent Concrete Properties Related to Design – Strength and Elastic Properties, Creep and Shrinkage," *Creep, Shrinkage and Temperature Effects*, SP-27, American Concrete Institute, Farmington Hills, MI, 257-277.

BSI (2004), *BS EN 1992-1-1: 2004, Eurocode 2: Design of concrete structures – Part 1-1: General rules and rules for buildings*, British Standards Institute, London.

CEB (1993), *CEB-FIP Model Code 1990*, CEB Bulletin d'Information No.213/214, Comité Euro-International du Béton, Lausanne, Switzerland.

CEB (1999), *Structural concrete – textbook on behaviour, design and performance. Updated knowledge of the CEB/FIP Model Code 1990*, fib Bulletin 2, V.2, Fédération Internationale du Béton, Lausanne, Switzerland, 37-52.

CEB/FIP (1983), *FIP Manual of Lightweight Aggregate Concrete* (2nd Edition), Surrey University Press, Glasgow and London.

Chia, K.S., Zhang, M.H. and Liew, J.Y.R. (2011), "High-strength ultra lightweight cement composite - material properties", *Proceedings of the 9th international symposium on high performance concrete-design, verification & ulitility*, Rotorua, New Zealand, August.

Gardner, N.J. and Lockman, M.J. (2001), "Design provisions for drying shrinkage and creep of normal strength concrete", *ACI Mat. J.*, **98**(2), 159-167.

Gardner, N.J. (2004), "Comparison of prediction provisions for drying shrinkage and creep of normal strength concretes", *Can. J. Civil Eng.*, **31**(5), 767-775.

Kwak, H.G., Ha, S.J. and Kim, J.K. (2006a), "Non-structural cracking in RC walls, Part I. Finitite element formulation," *Cement Concrete Res.*, **36**, 749-760.

Kwak, H.G. and Ha, S.J. (2006b), "Non-structural cracking in RC walls, Part II. Quantitative prediction model," *Cement Concrete Res.*, **36**, 761-775.

Lopez, M., Kahn, L.F. and Kurtis, K.E. (2004), "Creep and shrinkage of high-performance lightweight concrete", *ACI Mat. J.,* **101**(5), 391-399.

Sohel, K.M.A., Liew, J.Y.R., Yan, J.B., Zhang, M.H. and Chia, K.S. (2012), "Behavior of steel-concrete-steel sandwich structures with lightweight cement composite and novel shear connectors", *Compos. Struct.*, **94**, 3500-3509.